

Frank H. George Research Award Winning Paper

Cybernetic approach to medical technology: application to cancer screening and other diagnostics

Cybernetic
approach to
technology

871

D. Dutta Majumder and M. Bhattacharya
*Electronics & Communication Sciences Unit 1, Indian Statistical
Institute, Calcutta, India, and
Institute of Cybernetics Systems & Information Technology,
Salt Lake City, Calcutta, India*

Keywords Cybernetics, Medical, Diagnosis, Disease, Screening

Abstract The cybernetic approach differs significantly from the conventional reductionist methods of natural and biological sciences. Norbert Wiener established the theory of cybernetics as a science of control and communication process in living beings (human and animals) and machines. Dutta Majumder in his Norbert Wiener Award winning paper extended the approach to include integrated complex human machine systems and functions with general systems theory as a unitary science laying the mathematical foundation for unifying observing systems, observed systems and the act of observing as indicated in von Foerster's concept of second-order cybernetics. Both from the point of view of ontology and that of epistemology the cybernetic approach now enables computer technology to incorporate artificial intelligence (AI) and expert system (ES) for knowledge based instrumentation for diagnostics and therapy planning. Presents the results of a project for development of a knowledge based framework for combining different modalities of medical image processing such as CT, MR(T_1), MR(T_2), SPECT, PET, USG etc. whichever is relevant for particular pathological investigation for diagnostics and therapeutic planning. Experiments were conducted with (a) Alzheimer's patient data and (b) detection and grading of malignancy with oncological data for the cancer screening system.

1. Introduction and perspective

It is well-known that the development of cybernetics as a modern discipline with a distinctive influence on almost all branches of science and technology follows from Norbert Wiener's (1948) publication on the subject in 1948. The subject of cybernetics emerged through the interaction of traditional sciences when scientists and engineers faced a set of problems concerned with communication, control and computation in machines and living tissues. So one line leads to the study of automatic activity of living beings and the other line leads to that of machines including mechanization of intelligent activity including mathematical logic, artificial intelligence and related subjects of

The work is part of a project jointly funded by DST and CSIR, Govt of India. The authors wish to acknowledge with thanks AIIMS (All India Institute of Medical Science, Delhi), Eko Imaging Centre, Calcutta for providing data and consultation. We acknowledge with thanks the help and assistance rendered by our colleagues of the Indian Statistical Institute and Institute of Cybernetics Systems and Information Technology, Calcutta.

computer science and information technology. Whereas the above mentioned formalism of classical cybernetics was about "observed systems", H. von Foerster (1981) in his paper on second order cybernetics (SOC) enunciated about "observing systems". D. Dutta Majumder in his Norbert Wiener Award Winning paper (Majumder, 1979), "Cybernetics and general systems theory a unitary science" (Majumder, 1975, 1979; Majumder and Bhattacharya, 1999) combined the "observer systems", "observed systems" and the "act of observing" in the environment into one unitary holistic discipline of a general dynamical system from the points of view of perspective, motivation, requirements, characteristics, attributes and behaviour. In Dutta Majumder's mathematical formalism (Majumder, 1979), two important examples of attributes are the reproducibility and controllability of systems. In his generalisation he dealt with the problem of fundamental importance in nature, man, society and machines in developing a general theory of systems in terms of causality, signal predictability and the notion of state in dynamical systems. This is the essence of Dutta Majumder's theory of Cybernetic Approach to Medical Technology, which envisages "The Whole" (holistic) as a system while examining the minutest details of components of their relationships that constitute the whole namely integrated complex human-machine general systems (Majumder and Bhattacharya, 1999).

In post-Wiener cybernetics the subject has been developed to second order cybernetics which includes observation by an external observer and by the system upon itself and the outside world. The cybernetic approach enables medical technology with Artificial Intelligence and Expert System based computerised instrumentation for pathological study, diagnostics and therapeutic planning; a much better disease planning and patient management system at a much lower cost is realisable as the structural and functional information can have a reciprocal flow between the machines and living tissues. Computers not only have taken over normal signal analysis tasks such as ECG/ EEG/ EMG, Cytological/Histological applications, X-ray analysis, mass screening of diseases etc. but have contributed in the analysis of highly innovative observational technology in 3D images such as CAT, MRI, SPECT, PET, USG etc. The recent trend of research consists of combining more than one relevant modality for uncertainty management in diagnostics and therapeutic planning. In this paper we shall present some of the results of our work in the above mentioned areas of computer applications in medical technology (Majumder and Bhattacharya, 1997a, 1998a, 2000; Bhattacharya and Majumder, 1999).

It is now possible to have software programs which merge data from EEG or EMG or even PET or SPECT, USG and CT or MRI of the brain to yield a powerful new functional imaging technology.

2. Processing of medical images for therapeutic planning

Preprocessing of images is required before segmentation of region of interest (ROI), feature extraction and recognition (Chaudhuri and Majumder, 1984). The

processed images appear better in quality for diagnostics purposes and to distinguish more clearly the superimposed structures of the images.

For certain specific application the digital radiographs are modified by image enhancement and restoration to get more suitable results (Chanda *et al.*, 1984b; Bhattacharya and Majumder, 1996; Tahoves *et al.*, 1991; Steven *et al.*, 1977). Enhancement techniques convolve the grey level of a pixel independently of its neighbours using spatial masks. Enhancement includes image smoothing by two dimensional filtering of images, sharpening, edge detection and contrast stretching. Image segmentation is the process of localisation of the region of interest (ROI) in the image. This is particularly true in radiographic image analysis where one needs accurate outlines of an object which is not too clearly defined in the original image. Edge segmentation plays an important role in recognition as edges of images hold much information of the image to get the information of the shape, size and texture. In our works we have used different masks such as "Compass Gradient" or "Differential Edge Detector" known as Sobel, Kirsch, Prewitt, Robert and higher order differential as "Laplacian" (Chaudhuri and Majumder, 1984; Rosenfeld, 1970). We have also used modified higher order edge detection technique to demonstrate the effect of image processing on radiographic images (John, 1986). Different thresholding techniques are adopted for edge detection. We have also implemented the contrast based edge detection that arises when luminance values are unequal over the images.

Using selective masking on the chest radiograph, the bronchi, the cardiac area, the border of the heart and lung structures are clarified which is very important for diagnosing the quantitative measure of heart size and shape of heart which are the diagnostic signs of heart diseases. The processed radiographs of shoulder joint are useful to distinguish the inflammatory process around bone layer, around ball and socket joint (Bhattacharya and Majumder, 1996).

Restoration of biomedical images

Restoration is a process that attempts to reconstruct or recover an image that has been degraded by using some a priori knowledge of the degradation phenomena (Chaudhuri and Majumder, 1984; Chanda *et al.*, 1984a; Andrews and Hunt, 1977). The least square estimation technique has been implemented in image restoration technique and to improve the result the modified methods have been used which is called a constrained least square estimation (CLSE) (Chaudhuri and Majumder, 1984; Chanda *et al.*, 1984a). The criterion for optimality is used for the minimisation of the co-relation between the image and noise grey levels.

The Discrete Fourier Transform (DFT) algorithm has been implemented for the image restoration process which offers a considerable computational advantage over direct implementation of the Fourier transform. The degradation process is modelled as an operator H which together with an additive noise term $n(x,y)$ operates on an input image $f(x,y)$. Digital image restoration is the process of obtaining an approximation to $f(x,y)$, given $g(x,y)$ and a knowledge of the degradation in the form of the operator H :

metes

$$f(x, y) \rightarrow H \cdot g(x, y)$$

The additive noise term is $n(x, y)$, so the above equation is modified as

$$g = Hf + n.$$

f, g and n represent the same dimension of column vectors.

The objective of image restoration is to estimate an original image f from a degraded image g and some knowledge or assumption about H and n . This can be done within a unified linear framework. To find the solution for f the least squares criteria have been searched. These methods are the result of considering either an unconstrained or a constrained approach to least squares restoration problem. In unconstrained restoration, in the absence of any knowledge about n , a meaningful criterion function is to seek a value for f such that Hf approximates g in least squares sense by assuming that the norm of the noise term is as small as possible, whereas in constrained least square restoration problem the function of the form $|Qf|^2$ is to be minimised where Q is a linear operator on f , subject to the constraint. This approach introduces considerable flexibility in the restoration process because it yields different solutions for different choices of Q . The addition of an equality constraint in the minimisation problem is solved by using the method of Lagrange's multipliers. A constant α is used called Lagrangian multiplier.

The image restoration approach is commonly referred to as the inverse filter method. This terminology arises from considering $H(u, v)$ as a filter function that multiplies $F(u, v)$ to produce the transform of the degraded image $g(x, y)$. One of the most effective filtering techniques is Wiener Filter enunciated by Norbert Wiener which we have implemented for medical image restoration.

Wiener Filter and constrained least squares restoration

Let R_f and R_n be the correlation matrices of f and n defined respectively by the equations,

$$R_f = E \{ff^T\} \text{ and } R_n = E \{nn^T\}$$

Where $E(\cdot)$ denotes the expected value operation and f and n are the source and noise matrices respectively. The ij element of R_f is given by $E\{f_i f_j\}$ which is the correlation between the i th and j th elements of f . Similarly the ij element of R_n gives the correlation between the two corresponding elements in n . R_f and R_n are real symmetric matrices. Using A and B to denote matrices gives

$$R_f = WAW^{-1} \text{ and } R_n = WBW^{-1}$$

The elements A and B are the transform of the correlation elements in R_f and R_n respectively. The Fourier transform of these correlations is called power

spectrum (or spectral density) of $f_c(x,y)$ and $n_c(x,y)$ respectively and is denoted by $S_f(u,v)$ and $S_n(u,v)$:

$$Q^T Q = R^{-1} \gamma R_n$$

We have $\mathbf{g} = (\mathbf{H}^T \mathbf{H} + \gamma \mathbf{R}^{-1} \gamma \mathbf{R}_n)^{-1} \mathbf{H}^T \mathbf{g}$.

Therefore we have,

$$F'(u,v) = \left[\frac{H^*(u,v)}{\|H(u,v)\|^2 + \gamma [S_n(u,v) / S_f(u,v)]} \right] G(u,v) \dots$$

where $\|H(u,v)\|^2 = H^*(u,v) H(u,v)$ and it is assumed that $M = N$.

When $\gamma = 1$, the term inside the outer bracket in the above equation reduces to Wiener Filter. If γ is variable this expression is called the parametric Wiener Filter. In the absence of noise $S_n(u,v) = 0$ and the Wiener Filter reduces to the ideal inverse filter. For $\gamma = 1$ the solution is optimal in the sense that it minimises the quantity $E [f(x,y) - f'(x,y)]^2$.

When $S_n(u,v)$ and $S_f(u,v)$ are unknown this is approximated by the relation

$$F'(u,v) = \left[\frac{|H(u,v)|^2 G(u,v)}{|H(u,v)|^2 + K} \right] \dots$$

where K is a constant.

The least mean squares approach is a statistical approach because the criterion for optimality is based on the correlation matrices of the image and noise functions. This implies that the results obtained by using a Wiener Filter are optimal in an average sense. However, the restoration procedure considered here is optimal for each given image and requires knowledge only of the noise mean and variance.

The restoration solution depends on the choice of the matrix Q . Sometimes for ill-conditioning the solution may have large oscillating values and Q should be chosen in such a fashion as to minimise this adverse effect. The optimality criterion is based on a measure of smoothness by minimising some functions of the second derivative. Let us consider 1D case.

For a discrete function $f(x)$, $x = 0,1,2 \dots$ the second derivative at a point x may be approximated by the expression,

$$\frac{\partial^2 f(x)}{\partial x^2} = f(x+1) - 2f(x) + f(x-1).$$

This is the criterion to minimise the above expression to get a "smoothing" matrix and for 2D case we have to minimise the expression,

$$\left(\frac{\partial^2 f(x,y)}{\partial x^2} + \frac{\partial^2 f(x,y)}{\partial y^2} \right)^2$$

where the derivative function is approximated.

The derivative function can be implemented by convolving $f(x,y)$ with the operator,

$$p(x,y) = \begin{pmatrix} 0 & -1 & 0 \\ -1 & 4 & -1 \\ 0 & -1 & 0 \end{pmatrix}.$$

876

Wraparound error in the discrete convolution process is avoided by extending $f(x,y)$ and $p(x,y)$. $p_e(x,y)$ is formed as:

If $0 \leq x \leq 2$ and $0 \leq y \leq 2$ then

$$p_e(x,y) = p(x,y)$$

If $3 \leq x \leq M-1$ or $3 \leq y \leq N-1$

$$p_e(x,y) = 0$$

If $f(x,y)$ is of size $A \times B$, M and N is chosen as $M \geq A + 3 - 1$ and $N \geq B + 3 - 1$

For $p(x,y)$ of size 3×3 .

The convolution of the extended function is:

$$g_e(x,y) = \sum_{m=0}^{M-1} \sum_{n=0}^{N-1} f_e(m,n) p_e(x-m, y-n)$$

Smoothness criteria are expressed in the block circulant matrix of the following form and is constructed as,

$$C = \begin{pmatrix} C_0 & C_{M-1} & C_{M-2} & \dots & C_1 \\ C_1 & C_0 & C_{M-1} & \dots & C_2 \\ C_2 & C_1 & C_0 & & C_3 \\ \dots & \dots & \dots & \dots & \dots \\ C_{M-1} & C_{M-2} & C_{M-3} & & C_0 \end{pmatrix}$$

where each submatrix C_j is an $N \times N$ circulant constructed from the j th row of $p_e(x,y)$ that is,

$$C_j = \begin{pmatrix} p_e(j,0) & p_e(j,N-1) \dots \dots \dots p_e(j,1) \\ p_e(j,1) & p_e(j,0) \dots \dots \dots p_e(j,2) \\ \dots & \dots & \dots & \dots & \dots \\ p_e(j,N-1) & p_e(j,N-2) \dots \dots \dots p_e(j,0) \end{pmatrix}$$

Since C is block circulant it is diagonalised by the matrix W . That is,

$$E = W^{-1} C W$$

$P(u,v)$ is the 2D Fourier transform of $p_e(x,y)$; the smoothness criteria for 2D case take the form $f^T C^T C f$ where f is an MN dimensional vector and C is of size $MN \times MN$. Let $Q = C$ and from the equation

$$\|Qf\|^2 = f^T Q^T Q f$$

the criteria are expressed by minimising $\|Qf\|^2$ and with $Q = C$ the optimal solution is given by,

$$f' = (H^T H + \gamma C^T C)^{-1} H^T g \dots$$

$$H = W^* D W^{-1} \text{ and } H^T = W D^* W^{-1}$$

The equation can be expressed as,

$$f' = (W D^* D W^{-1} + \gamma W E^* E W^{-1})^{-1} W D^* W^{-1} g.$$

Multiplying both sides by W^{-1} we have,

$$W^{-1} f' = (D^* D + \gamma E^* E)^{-1} D^* W^{-1} g \dots$$

So,

$$F'(u,v) = \left[\frac{|H^*(u,v)| G(u,v)}{|H(u,v)|^2 + \gamma |P(u,v)|^2} \right]$$

for $M = N$, $|H(u,v)|^2 = H^*(u,v) H(u,v)$.

γ is so adjusted that it should satisfy the constraint $\|g - Hf'\|^2 = \|n\|^2$

The solution of the above equation can be optimal only when γ satisfies the condition. An iterative procedure for estimating the parameter is as follows: let r be a residual vector defined as,

$$r = g - Hf' \dots$$

substituting f'

$$r = g - H (H^T H + \gamma C^T C)^{-1} H^T g \dots$$

The above equation indicates that r is a function of γ and it is a monotonically increasing function. Adjusting γ we get $\|r\|^2 = \|n\|^2 \pm a \dots$ where a is the accuracy factor. If $\|r\|^2 = \|n\|^2$ the constraint $\|g - Hf'\|^2 = \|n\|^2$ will be strictly satisfied.

To determine γ the following steps are considered:

- (1) to specify an initial value of γ
- (2) to compute f' and $\|r\|^2$
- (3) the process continues increasing γ if $\|r\|^2 < \|n\|^2 - a$ or decreasing γ if $\|r\|^2 > \|n\|^2 + a$.

Knowledge of $\|n\|^2$ is required to implement the above steps.

The variance of $n_e(x,y)$ is given by,

$$\sigma_n^2 = E[n_e^2(x,y)] - n_e'^2 \dots$$

where, $n_e' = \frac{1}{(M-1)(N-1)} \sum \sum n_e(x,y) \dots$

Where n_e' is the mean value of $n_e(x,y)$, if a sample average is used to approximate the expected value of $n_e^2(x,y)$, the equation becomes,

where $\sigma_n^2 = \frac{1}{(M-1)(N-1)} \sum \sum n_e^2(x,y) - n_e'^2$.

The summation term simply indicates squaring and adding all values in the array $n_e(x,y)$, $x = 0,1,2 \dots M-1$ and $y = 0,1,2 \dots N-1$.

Hence the above equation reduces to,

$$\sigma_n^2 = \frac{||n^2||}{(M-1)(N-1)} - n_e'^2 \dots$$

or, $||n^2|| = (M-1)(N-1)[\sigma_n^2 + n_e'^2] \dots$

The importance of this equation lies in the fact that it allows the determination of a value for the constraint in terms of the noise mean and variance. This gives the idea for restoration process using least square estimation method.

Q is taken as a block circulant matrix. If the noise terms are zero uncorrelated, a straightforward analysis leads to

$$Q^T Q = \frac{1}{M^2} S_n I \dots$$

Where I is the identity matrix

$$\text{and } S_n = \frac{1}{M^2} \sum_{i=0}^{M-1} \sum_{j=0}^{N-1} n_e^2(i,j) = \sigma_n^2 \dots$$

σ_n^2 is the variance of the noise grey levels and we get

$$F_e'(u,v) = \frac{H(u,v) G_e(u,v)}{H^2(u,v) + \gamma S_n} \dots$$

$F_e(u,v)$ and $G_e(u,v)$ are the (u,v) th coefficients of two-dimensional Fourier transform of $f_e'(i,j)$ and $g'(i,j)$ respectively.

Results and discussions

The restoration techniques are implemented on human brain images having space occupying tumor lesion using CT modality. A small rectangular portion of the entire picture is taken by the windowing process which satisfies the condition that the background of the extracted portion has a uniform grey level. The size of the extracted portion has been extended on both dimensions accordingly. The improvement of the signal to noise ratio of the image is the measure of the performance of the filters. In the experiment Gaussian-shaped

point spread function (PSF) is used to blur the source image. The images are blurred by defocusing using different values of (γ) starting from zero and finally restored using Wiener Filter method. It can be concluded that the restoration method using CLSE method is the best followed by Wiener Filter method and lastly inverse filtering technique.

An objective measure of performance, the improvement in the signal to noise ratio (ISNR) has been used. It is defined by:

$$ISNR = 20 \log \left\{ \frac{\|f\|^2}{\|f - f'\|^2} \right\}$$

where f and f' are the original and the estimated signal respectively. For the blur a Gaussian shaped PSF is used which is given by

$$h(i, j) = c \exp \left\{ -\frac{i^2 + j^2}{2\sigma^2} \right\}$$

for $i, j = 0, 1, 2, \dots, M - 1$ where c is a constant ensures a lossless system. That is

$$\sum_{i,j} h(i, j) = 1$$

In the experiment the Gaussian Shaped PSF is used to blur the source image of variance $\sigma^2 = 6.25$.

The original defocused picture contains small noise due to granularity in the overlapping paper. Figure (1a) shows the original CT image. Figure (1b) shows

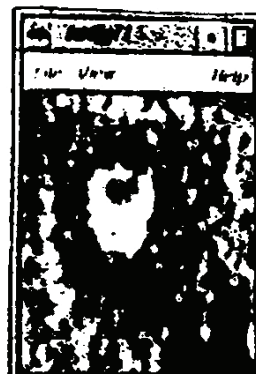


Figure 1a.
Original image of brain
tumour of size 128×128

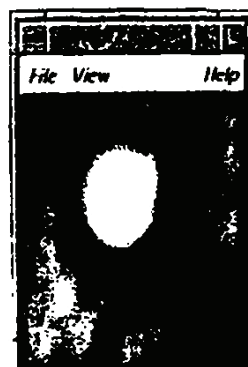


Figure 1b.
Image blurred and
corrupted by additive
noise

the blurred image obtained by applying the Gaussian PSF operator on the original image. Figure (1c) shows the result of using inverse filtering technique ($\gamma = 0$). The ill-conditioned nature of the solution is evident by the dominance of the noise on the restored nature.

Figure (1d) shows the restored image using Wiener Filter method. Figures (1e), (1f), (1g) are the restored images of the defocused image using value of γ as $\gamma = 0.018$, $\gamma = 0.010$ and $\gamma = 0.008$ respectively (CLSE method).

Figure 1c.
Filtering technique

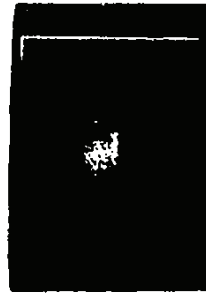


Figure 1d.
Image restored using
Wiener filtering
technique

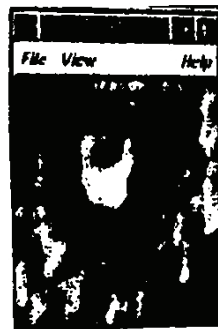


Figure 1e.
Image restored using
CLSE where $\gamma = 0.018$



Figure 1f.
Image restored using
CLSE where $\gamma = 0.01$



Figure 1g.
Image restored using
CLSE where $\gamma = 0.08$



For the images restored from the constrained least square estimation the accuracy factor "a" was chosen so that $a = 0.025 \sqrt{\|n\|^2}$. The improvement of the constrained solution over direct inverse filtering is clearly visible. Parameters that affect the outcome of a restoration are (a) signal to noise ratio; (b) shape and extent of the point spread function; (c) correlation properties of both the image and noise; (d) the optimality criteria chosen for restoration; (e) the extent and nature of the available a priori information.

The CLSE requires the least a priori information amongst the three methods described requiring the PSF only; noise variance is required but can be estimated from the degraded image. The Wiener Filter requires the most a priori information: the PSF and correlation functions of signal and noise. Visual quality is best for CLSE, next comes Wiener Filter and lastly inverse filtering.

Finally, we may conclude that restoration is a very complex subject in image processing techniques. One has to recognise the factors causing the degradation of an image and to choose the restoration technique to be applied on the image. It is mainly a trial and error method and a need exists to develop the methodologies for minimisation of this uncertainty. The next important factor is the right choice of the operator to be applied on the degraded image to recover the original image specially for biomedical images where degradation of images occur due to scattering, non-uniform exposure and other factors due to the apparatus.

3. A new approach for decision making in oncology

We have undertaken the task of developing screening test for detection and gradation of malignancy and benignancy in the following groups of tumours:

- (1) tumours in central nervous system appearing in brain as space occupying lesion;
- (2) tumour growth in breast region.

The classification technique is based on boundary detection of lesion using 2D shape metric analysis. In classification the ideas of "shape similarity" and "shape distance" (see Parui and Majumder, 1982, 1983; Majumder and Bhattacharya, 1997a, 1998a,b,c) are introduced using structural description applied for recognition of two-dimensional objects. The low degree of similarity predicts the tendency of growth to be malignant and high degree of similarity predicts the benignancy of tumour lesions. Computer assisted screening procedure might be useful for improved therapy planning by determining the accurate pre-operative stages for surgical procedure (Majumder and Bhattacharya, 1997a, 1998a,b,c,d).

A new approach to classification and gradation of tumours

"Shape" of an object is described on the basis of its structural features using certain chain codes. A description is information preserving in the sense that it is possible to reconstruct any reasonable approximation of the shape from the descriptor. The two reference points on the border of a region are defined which

are invariant under translation, dilation and rotation of the region (Parui and Majumder, 1982,1983; Majumder and Bhattacharya, 1998c). From these two reference points some strings of directional codes describing the border are extracted. For the extracted boundary the two basic considerations are "connectedness" and "closedness" subset of Euclidean plane R^2 . The reference points of a region belonging to equivalence class are unique and do not depend upon the position, size and orientation of same shape.

Extraction of feature of the boundary

The extracted border is represented by string number or directional code; d defines a direction that makes an angle $(i - d) 45^\circ$ with direction I where d is any real number lying between 1 to 8 and $i = (1, 2, \dots, 8)$. Let $d1 = (d1j)^n$ $j = 1$ be the contour representation starting from each reference point 1 and 2 and are denoted by $d1$ and $d2$ such that $d = (d1, d2)$ is the extracted feature from the region for two reference points described. The distance function D is derived on the basis of feature d .

The possible directional codes are $d1$ and $d2$ for a length of a contour having n number of points. If $d2$ is a rotation of $d1$ then $d2 = d1 + \gamma$ for any real number γ when

$$d2j = d1j + \gamma \text{ for all } j.$$

From the direction code representation the distance function D is computed for each reference position for $l = 1, 2$ between the contours to be matched, one being the model contour and another one the contour or region of interest in the image. The distance function D is defined in terms of two string numbers d^1 and d^2 belonging to a set as,

$$D(d1, d2) = \sum_{j=1}^n \min((d1j - d2j), 8 - (d1j - d2j))$$

The distance function D is computed in terms of string number between the two contours.

The normalised value of D^* is D^*/n and the shape similarity measure between the two shapes is given by,

$$\mu = 1 - D^*/n$$

Experiment: cancer screening using image analysis

We have implemented the shape based methodology for tumour classification of tumour lesions appearing in the Central Nervous System (CNS) located in the brain using CT and MR images and also implemented to detect the tumour lesion and to classify the lesions as being in the benign or malignant group using mammographic images.

Experimental results

We have experimented with five cases of tumours appearing in the brain as space occupying lesion using CT and MR images of the brain. In Figures 2-6.



Figure 2.
CT image of brain
shows benign cyst



Figure 3.
CT image of brain
shows malignant
tumour lesion



Figure 4.
CT image of brain shows
benign tumour lesion
with oedema effect

Figure 5.
MR image of brain
shows benign tumour
lesion



Figure 6.
MR image of brain
shows benign tumour
lesion



five cases of human brain tumours are shown. The segmented tumour lesions and the contours are shown in respective Figures 7-16. In Table I the gradation of benignancy or malignancy of the tumor growth in the brain and in Table II the tumour growth in the mammary gland are demonstrated from the computed value of "shape similarity measure" from which the decision can be made by the clinicians to take any preoperative procedures.

In the present study lesions having a μ value of less than 0.5 are detected to be malignant in nature and those having a μ value greater than 0.5 are benign in nature. We have also found a new gradation technique of the benignancy of the lesion. Lesions having a μ value lying from 1 to 0.9 are in grade 1, in between 0.9 to 0.8 lesions are in grade 2, for a μ value in between 0.8 to 0.7 the lesions are in grade 3, in between 0.7 to 0.6 the lesions are in grade 4 and in between 0.6 to 0.5 are in grade 5. Higher grades of transformation indicate the tendency of the tumour growth towards malignancy. For case I the degree of benignancy of tumour growth is the highest order compared to the other cases. So the lesion is benign in nature and risk factor is lowest compared to the other cases. The μ values for case II, case III and case V also indicate the benignancy of tumour growth but the tendency of growth for case III and case V towards

malignancy is higher than case I and case II; as a result the risk factor for case III and case V is higher than case I and case II. The μ value for case IV indicates the tumour lesion to be completely malignant in nature.

The objective of this study is to find a new classification system for tumour growth enabling different levels of gradation from coarse to fine which may be clinically useful for the medical practitioners to take decisions.



Figure 7.
Segmented cyst image



Figure 8.
Segmented tumour lesion

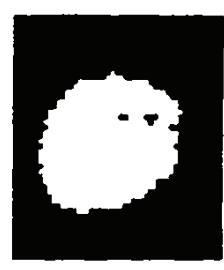


Figure 9.
Segmented tumour lesion



Figure 10.
Segmented tumour lesion



Figure 11.
Segmented tumour lesion

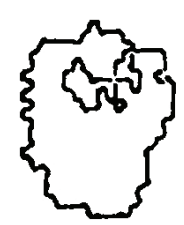


Figure 12.
Contour of cyst

4. Multimodal image registration and fusion

The registration solves the correspondence problem of the respective modalities and fusion performs the integration of information to a single reference frame. The registration was performed using theory of shape (Majumder, 1995; Majumder and Bhattacharya, 1998a, 1999, 2000) and fusion was performed using the Dempster-Shafer Evidence Accumulation Theory (Majumder and Bhattacharya, 1997b, 1998d,f; Bhattacharya and Majumder, 1994; Shafer, 1996; Bloch, 1994).

Registration of multimodal medical images

The registration and matching of three modality images CT, T_1 weighted MR and T_2 weighted MR images of the axial section of human brain of an Alzheimer's patient (de Leon *et al.*, 1989; Arai *et al.*, 1983) have been achieved. A knowledge based framework has been developed to combine different modality medical images for pathological and anatomical investigations. The methodology developed is based on 2D shape analysis and non-rigid shape matching of objects in specified transformation planes.

A new generalised approach has been developed for registration between two sets of landmark points representing two shapes. The two sets are superimposed

Figure 13.
Contour of tumour
lesion



Figure 14.
Segmented tumour
lesion

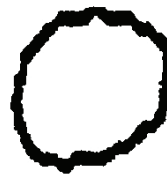
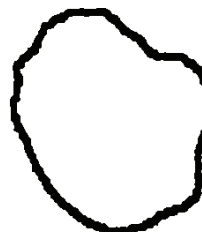


Figure 15.
Contour of tumour
lesion



Figure 16.
Contour of tumour
lesion



by translating, scaling or rotating. If exact superimposition is not possible then the closest match is found by employing the new methodology. The contour of the ROI (ventricular region) is detected by using Canny edge segmentation (Canny, 1986) algorithm. An appropriate co-ordinate transformation is considered so that one set of landmark points can be mapped on to the other. The co-ordinates are expressed as a Taylor series expansion. The polynomial series consists of two parts:

- (1) an affine part;
- (2) a nonlinear part.

An affine transformation is related to translation, rotation and scaling. Scaling is essential to define the shape distortion.

In canonical frame the affine invariants (Majumder and Bhattacharya, 1998a, 2000; Mundy and Zisserman, 1993; Van den Elsen *et al.*, 1993) are determined from the entry, exit and height point of the concavity of the contour. When two images are under an affine, two-dimensional transformation each point m in one image is translated to a corresponding point given by

$$m' = Cm + d$$

where C is a nonsingular 2×2 matrix and d is the translational vector. In the required canonical frame the non-colinear triplet of model points is transformed to a co-ordinate position $(-100,0); (100,0); (0,100\sqrt{3})$.

The generalised expression for transformation matrix is given by,

$$\begin{pmatrix} x_c \\ y_c \end{pmatrix} = \begin{pmatrix} p & q \\ s & t \end{pmatrix} \begin{pmatrix} x_t \\ y_t \end{pmatrix} + \begin{pmatrix} r \\ u \end{pmatrix}$$

Case	Measure of μ	Tendency of tumour growth	Nature of tumour	Grade of benignancy
I	0.72	Benign	Intracranial cyst	Grade 3
II	0.59	Benign	Primary neoplasm	Grade 5
III	0.56	Benign	Glioma	Grade 5
IV	0.41	Malignant	Primary neoplasm	-
V	0.65	Benign	Lesion with oedema effect	Grade 4

Table I.
Gradation of
benignancy or
malignancy of tumour
lesion from shape
similarity measure (μ)

Case	Measure of μ	Grade	Tendency of growth
I	0.94	I	Benign
II	0.82	II	Benign
III	0.67	IV	Benign
IV	0.32	-	Malignant
V	0.7	III	Benign

Table II.
Gradation of
benignancy or
malignancy for tumour
growth in mammary
glanc

The six degrees of freedom are specified by the parameters p,q,r,s,t,u in affine plane to map the chosen concavity in the canonical frame. Here x_t and y_t are detected from convex hull method and are the hullpoints of the corresponding concavity of the contour and x_c and y_c are the corresponding control points in the canonical frame.

A projective transformation can be represented between two planes as (Majumder and Bhattacharya, 1998a, 2000; Mundy and Zisserman, 1993):

$$x = TX^t$$

Any planar transformation of homogeneous co-ordinates defines a projective transformation of the projective plane. A point in the projective plane can be presented by three co-ordinates as $(x_1, x_2, x_3)^t$ and these are called homogeneous co-ordinates. In the projective plane of three homogeneous co-ordinates the transformation is expressed by a 3×3 matrix and the eight degrees of freedom are specified by the parameters in a nine-dimensional space defined by all the matrix elements. Mathematically this transformation is presented in the canonical frame as,

$$\begin{pmatrix} x_c \\ y_c \\ 1 \end{pmatrix} = \begin{pmatrix} a & b & c \\ d & e & f \\ g & h & 1 \end{pmatrix} \begin{pmatrix} x_t \\ y_t \\ 1 \end{pmatrix}$$

Results and discussion

In both the affine and projective planes the matching between the extracted contour of CT, T_1 and T_2 weighted MR images of an Alzheimer's patient are estimated following the 2-D shape matching algorithms. The transformation is done along the upper concavity of the ventricular region; the same transformation has been implemented considering the lower concavity. The projective transformation is applied on the images.

The section of brain images of an Alzheimer's patient is shown in Figure 17 using T_1 weighted MR, T_2 weighted MR and CT imaging modalities. The dilation of the ventricular region is one of the determining clinical features for Alzheimer's patient. In the present experiment the ventricular region of each image has been taken as the region of interest (ROI).

5. Multimodal image fusion using soft computing methods

The combination of information from the multimodal imageries as a fused image would provide the optimum information (Hall, 1998). The multimodal medical image fusion may provide integrated information to the medical practitioners for improved diagnostics and therapeutic planning (Majumder and Bhattacharya, 1997b, 1998d,e,f, 1999). The objective is to indicate an approach based on soft computing methods in uncertainty management for decision making in context dependent and context independent systems of data fusion for medical images. However, the four major classes of data fusion



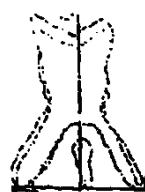
T_1 weighted MR Image
of brain of an AD patient



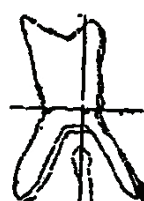
T_2 weighted MR Image
of brain of same patient



CT image of brain
of same patient



Registered T_1 & T_2 weighted
MR images of brain in the
Ventricular region
(affine transformation)



Registered T_1 & T_2 weighted
MR images of brain in the
ventricular region (projective
transformation)



Registered T_1 , T_2 and CT
images of brain in the
ventricular region

Figure 17.
Images of the brain

operators used or recommended (Majumder and Bhattacharya, 1997b, 1998d,e,f) for multisensor images are:

- (1) Probabilistic and Bayesian Theory.
- (2) Fuzzy Sets and Possibility Theory.
- (3) MYCIN like Pseudo Probabilistic Systems.
- (4) Dempster-Shafer Evidence Accumulation Theory (Shafer, 1996; Majumder and Bhattacharya, 1997b, 1998(d,e,f); Bloch, 1994).

We have implemented some information combination operators and some aspects of Dempster-Shafer Evidence Accumulation theory for classification of multimodal images. In medical image fusion the diagnostics capability is improved by reducing the detection of false diagnostics criteria. In data fusion systems the numerical or symbolic information extracted from images or sensors is represented as a measure of belief in an event. In the presentation of information the inherent uncertainties, impreciseness and incompleteness in connection with observation, acquisition are taken into account. The degrees of belief measure mentioned take generally their values in a real closed interval of $([0,1] \cup [-1,1] \dots)$ and are modelled after a different mathematical framework. In the present work we have developed the fusion operator based on the Dempster-Shafer theory of accumulation of evidences to combine the T_1 weighted MR and T_2 weighted MR images of brain.

Dempster-Shafer model used for fusion of medical images

Let the frame of discernment θ be the set of all elementary propositions $m(\theta)$ which is the probability mass function indicating to what extent a sensor is able to distinguish any elementary proposition. From the concept of probability mass m another two functions are defined which are an evidential interval and denoted by belief and plausibility measures. Belief for a proposition S_i is defined by the equation,

$$\text{Bel } S_i = \sum_{S_j \in \theta, S_j \subseteq S_i} m(S_j)$$

where $S_i = A_1 \cup A_2 \cup A_3$, where A_1, A_2, A_3 are the three classes defined in the problem.

Combination of probability masses as,

$$\text{bel}(A_1 \cup A_2 \cup A_3) = m(A_1) + m(A_2) + m(A_3) + m(A_1 \cup A_2) + m(A_2 \cup A_3) + m(A_1 \cup A_3) + m(A_1 \cup A_2 \cup A_3)$$

and the plausibility measure $\text{pls}(P_i)$ is simply $\text{pls}(P_i) = 1 - \text{bel}(\neg S_i)$.

Thus from the D-S theory a number in the interval $[0,1]$ is used which indicates the degree of evidence to support a proposition. Thus $m:2^\theta \rightarrow [0,1]$ and $\sum m(A) = 1$ for all A contained in θ and similarly the null hypothesis is assigned as $m(\emptyset) = 0$ such that the subset A of the frame of discernment θ is the focal element having all non-zero probability mass value:

$$\text{bel}(S) = \sum m(A), \text{ for all } A \text{ contained in } S \text{ and } \text{pls}(S) = \sum \{A \cap B \neq \emptyset\} m(A).$$

The two images Im1 and Im2 are complementary to each other. By D-method of fusion the probability masses are assigned in a area where the union of classes defined is mixed.

Experimental procedure and result

In image1 (Figure 18a) and in image2 (Figure 18b) the classes are discriminated in:

- (1) grey matter;
- (2) white matter;
- (3) cerebrospinal fluid (CSF);
- (4) ventricle; and in
- (5) bones.



(a) Image1 (Im1)



(b) Image2 (Im2)



(c) Fused Image

Figure 18.
Fusion of medical
images

The grey matter and the white matter together constitute the brain region and according to our notation this is class C_1 , while the ventricle and CSF together are denoted by C_2 . The overlapping regions of C_1 and C_2 is denoted by $C_1 \cup C_2$ as C_3 and the outer bony layer of each slice are denoted by C_4 . So the four classes of brain matter are defined as C_1, C_2, C_3, C_4 . To assign the probability masses for each class a central or focal element is chosen. This central element is related to each class of the $Im1$ and $Im2$. The null mass $m(0)$ is defined for each class which is not assigned. To determine the probability masses the frame of discernment is proposed as $\theta = (C_1, C_2)$. The power set $2^\theta = (\theta, C_1, C_2, C_1 \cup C_2)$. The mass functions are assigned for two images as m_1 and as m_2 respectively and mass functions assigned for each class as $m_1(C_1), m_1(C_2), m_1(C_1 \cup C_2)$ for $Im1$ and as $m_2(C_1), m_2(C_2), m_2(C_1 \cup C_2)$ in $Im2$, such that, $m(C_1) + m(C_2) + m(C_1 \cup C_2) = 1$ And $bel(C_1) = m(C_1)$ and $bel(C_2) = m(C_2)$, $bel(C_1 \cup C_2) = m(C_1) + m(C_2) + m(C_1 \cup C_2) = 1$.

In pixel based classification the distribution of different pixels over a specified grey level is considered. In $Im1$ the pixels are spread over the range 20 to 190. Primarily we have considered the distribution of pixels over the ranges below 130, in between 130-190 and above 190.

When M is the number of pixels lying in the region over a specified grey level and if N is the dimension of the region ($N = N_1 \times N_2$) taken as a small image of the brain:

- (1) for pixels having grey values less than 130, $m_1(C_2) = 1, m_1(C_1) = 0$ and $m_1(C_1 \cup C_2) = 0$;
- (2) for pixels with grey level values greater than 190, $m_1(C_1) = 1, m_2(C_2) = 0, m_1(C_1 \cup C_2) = 0$;
- (3) for pixels with grey level values between 130 and 190, $m_1(C_1) = 0.49; m_1(C_2) = 0.3$ and $m_1(C_1 \cup C_2) = 0.193$.

Similarly for image2 $IM2$ the range of grey levels distributed over the pixels;

- (1) for pixels having grey values less than 90, $m_2(C_1) = 1, m_2(C_2) = 0, m_2(C_1 \cup C_2) = 0$.
- (2) for pixels having grey values 90 to 135, $m_2(C_2) = 0, m_2(C_1) = 0.552, m_2(C_1 \cup C_2) = 0.498$.
- (3) for pixels having grey values 135 and 140, $m_2(C_1) = M' / N', m_2(C_2) = M_1' / N_1'$ and $m_2(C_1 \cup C_2) = 1 - M' / N' + M_1' / N_1'$, thus $m_2(C_1) = 0.01, m_2(C_2) = 0, m_2(C_1 \cup C_2) = 0.99$.
- (4) for 140 to 197 range $m_2(C_1) = 0.03, m_2(C_2) = 0.07$ and $m_2(C_1 \cup C_2) = 0.9$.
- (5) between 197 and 255, $m_2(C_1) = 0, m_2(C_2) = 0.9$ and $m_2(C_1 \cup C_2) = 0.7$

The pixels at the specified grey value ranges are classified from both the images of the T_1 and T_2 weighted MR images of brain and are fused after the registration in a common reference frame using Dempster-Shafer accumulation Theory. The fused images of both the modalities are shown in Figure 18c. For a

pixel the decision is taken in favour of either C_1 or C_2 as to whether $bel(C_1) > bel(C_2)$ or vice versa. Thus the belief measure indicates in which class a pixel belongs in the fused image (Figure 18c).

6. Epistemological and ontological approach for development of medical expert systems

Development of a medical expert system is a very complex problem as medicine is a complex domain. The key problems are (a) defining general system architectures in terms of generic tasks such as diagnosis, therapy planning and monitoring to be executed for (b) medical reasoning in (a), (c) patient management (d) minimum uncertainty. The other problems are (e) knowledge acquisition and encoding, (f) human machine interface, (g) system integration into clinical environments. We have attempted to investigate these problems from a theoretical and computational point of view in the area of oncology.

Figure 19 shows the block diagram for environment of Expert System Development and Figure 20 shows a schematic representation of the Generate and Test model of Medical Reasoning System. An epistemological analysis focuses on the conceptual features of the high level domain and inference procedure knowledge that can be understood in terms of ontology and inference model. Abduction, deduction and induction represent the basic elements of the inference model of medical reasoning as shown in Figure 20. First a patient's clinical data are used to generate plausible hypotheses, then

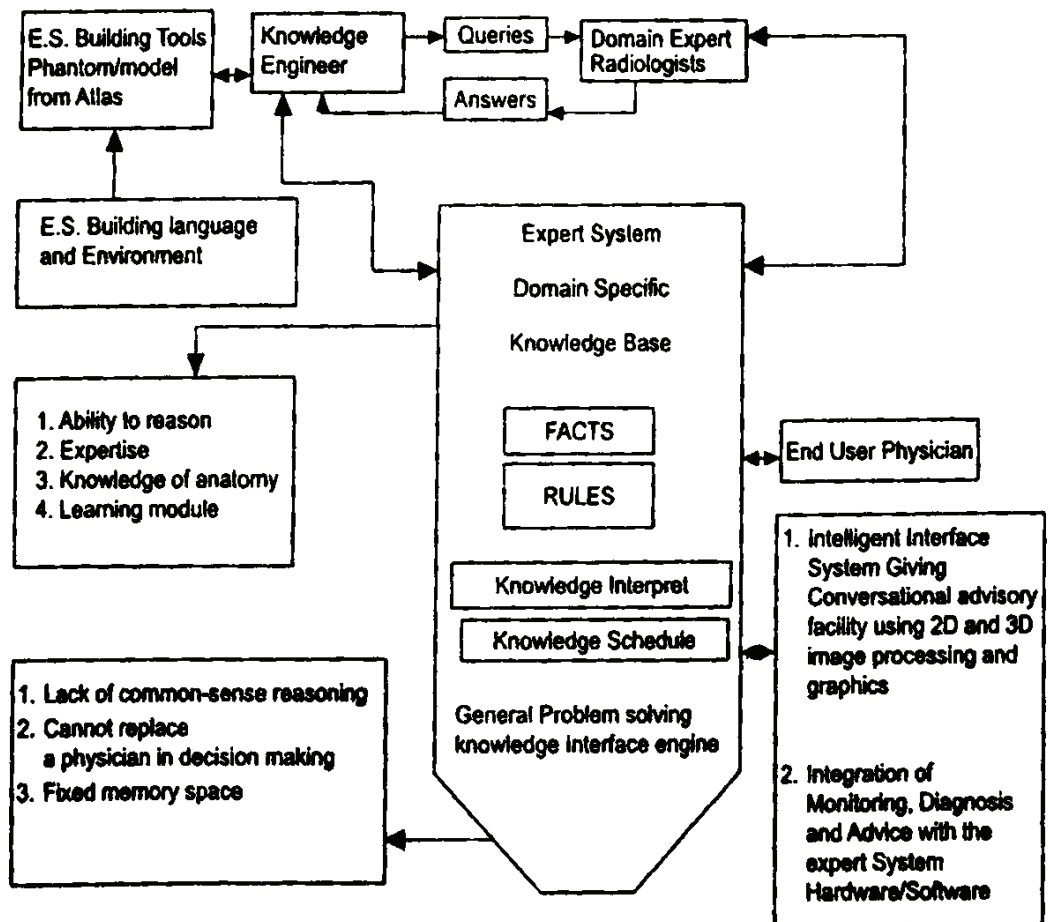


Figure 19. Diagram indicating expert system (ES) environment

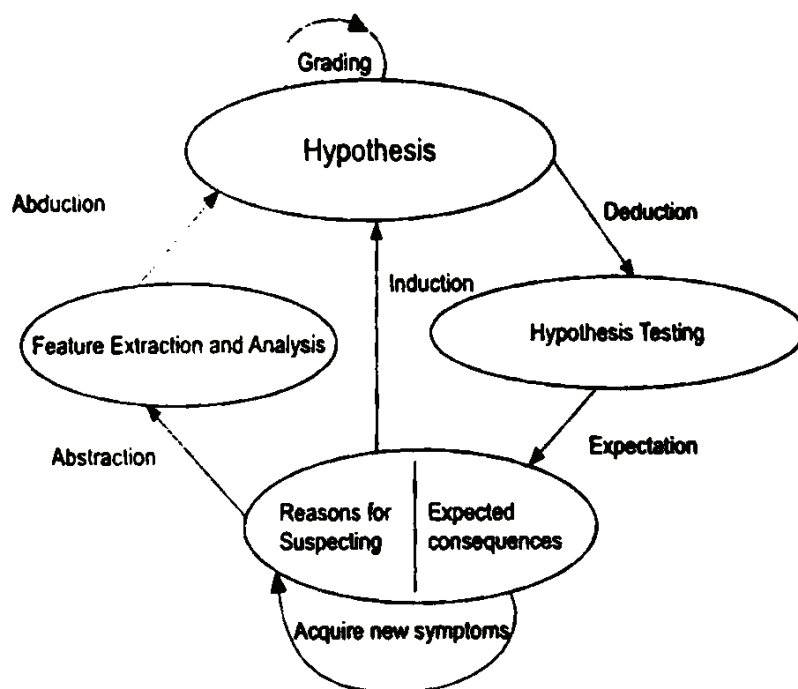


Figure 20. A schematic representation of the generate and test model of medical reasoning

these are used as starting conditions to forecast expected consequences which should be matched with the state of affairs of the patient in order to confirm or deny these hypotheses.

The complex tasks executed in medical reasoning are to be carried out in the generic tasks of:

- (1) Diagnostics adviser;
- (2) Therapy adviser;
- (3) The monitor; and
- (4) The patient manager.

References and further reading

- Andrews, H. and Hunt, B. (1977), *Digital Image Restoration*, Prentice-Hall, Englewood Cliffs, NJ.
- Arai, H. and Kobasaki, K. *et al.* (1983), "A computed tomography study of Alzheimer's disease", *J. Neurol.*, Vol. 229, pp. 69-77.
- Bhattacharya, M. and Majumder, D.D. (1996), "A study on application of digital image processing and pattern recognition in conventional radiographic images", ECSU-ISI Technical Report.
- Bhattacharya, M. and Majumder, D.D. (1998), "Breast cancer screening using mammographic image analysis", *16th International CODATA Conference*, 8-12 November, Delhi.
- Bhattacharya, M. and Majumder, D.D. (1999), "Multi resolution medical image registration using mutual information and shape theory", *Proceedings of 4th International Conf. on Advances in Pattern Recognition and Digital Techniques, ICAPRDT '99*, 28-31 December.
- Bloch, I. (1994), "Information combination operators for data fusion: a comparative review with classification", *IEEE Trans. Systems, Man, and Cybernet.*, pp. 26, 52-67.
- Canny, J. (1986), "A computational approach to edge detection", *IEEE Trans. on Pattern Analysis and Machine Intelligence Unit*, Vol. Pami-8 No. 6, November.

- Chanda, B., Chaudhuri, B.B. and Majumder, D.D. (1984a), "An efficient least square estimation technique for image restoration using image-noise correlation constraint", *IEEE Trans. Syst. Man. and Cybernet.*, Vol. 14, pp. 515-19.
- Chanda, B., Chaudhuri, B.B. and Majumder, D.D. (1984b), "Some algorithms for image enhancement incorporating human visual response", *Pattern Recognition*, Vol. 17, No. 4.
- Chaudhuri, B.B. and Majumder, D.D. (1984), *Two-Tone Image Processing and Recognition*, Wiley Eastern Limited, pp. 1-63, 88-100.
- de Leon, M.J. and George, A.E. *et al.* (1989), "Alzheimer's disease: longitudinal CT studies of ventricular change", *AJNR*, Vol. 10, pp. 371-8.
- Hall, D.L. (1998), *Mathematical Techniques in Multisensor Data Fusion*, Artech House, Boston, MA.
- Majumder, D.D. (1975) "Cybernetics, a science of engineering and biology", *Cybernetika*, Vol. xviii No. 3, International Association of Cybernetics, Namur (Belgium).
- Majumder, D.D. (1979), "Cybernetics and general system theory: a unitary science", *Kybernetes*, Vol. 8, pp. 7-15.
- Majumder, D.D. (1984), "Post-Wiener cybernetics", *6th International Congress of Cybernetics and Systems (WOSC)*, 10-14 September, AFCET, Paris, pp: xxxv-xl.
- Majumder, D.D. (1995), "A study on a mathematical theory of shapes in relation to pattern recognition and computer vision", *Indian Journal of Theoretical Physics*, Vol. 43 No. 4, pp. 19-30.
- Majumder, D.D. and Bhattacharya, M. (1997a), "A shape based approach to automated screening of malignancy in tumours in tomography and other related images", *IFTE Conf. NASELSOM*.
- Majumder, D.D. and Bhattacharya, M. (1997b), "Uncertainty management in multimodal image fusion system for diagnosis and therapy planning". *International Conference on Recent Advances in Statistics and Probability (Indian Statistical Institute & Bernoulli Society for Mathematical Statistics and Probability)*, Calcutta, 29 December - 1 January.
- Majumder, D.D. and Bhattacharya, M. (1998a), "A new shape based technique for classification and registration: application to multimodal medical images", *Int. J. of Image Processing and Communication*, Vol. 4 No. 3-4, pp. 45-70.
- Majumder, D.D. and Bhattacharya, M. (1998b), "A multimodal medical imaging processing system for diagnosis and therapy planning", *Intl. Conf. on Computers and Devices for Communication*, 4-17 January, Calcutta, India (CODEC).
- Majumder, D.D. and Bhattacharya, M. (1998c), "A multimodal medical image processing system for therapeutic planning", *Silver Jubilee Conference of Society of Management Science and Applied Cybernetics*, 12-13 January, (SCIMA), Vol. 25, (Silver Jubilee Special Issue) pp. 45-72.
- Majumder, D.D. and Bhattacharya, M. (1998d), "Soft computing methods for uncertainty management in multimodal image registration and fusion problems", *Intl. Conf. of Information Sciences JCIS -98, October, for oral presentation and in Proceedings*, Duke University, North Carolina, USA.
- Majumder, D.D. and Bhattacharya, M. (1998e), "Soft computing methods for uncertainty management in multimodal medical image data fusion", *16th International CODATA Conference*, 8-12 November, Delhi.
- Majumder, D.D. and Bhattacharya, M. (1998f), "Multimodal data fusion for Alzheimer's patients using Dempster-Shafer theory of evidence", *3rd Asian Fuzzy Systems Symposium*, Korea, Published in *Proceedings*, pp. 713-19.
- Majumder, D.D. and Bhattacharya, M. (1999), "Cybernetic approach to medical technology for diagnosis and therapy planning", *Proceedings of 11th International Congress of*

Cybernetics and Systems, World Organisation of Systems and Cybernetics, August, Brunel University, Uxbridge, Middlesex, pp. 103-08.

Majumder, D.D. and Bhattacharya, M. (2000), "Registration of multiview images of Alzheimer's patient: a shape theoretic approach", *Accepted Pattern Recognition Letters*, Elsevier Publications.

Mundy, J.L. and Zisserman, A. (Eds) (1993), *Geometric Invariance in Computer Vision*, The MIT Press, Cambridge, MA.

Parui, S.K. and Majumder, D.D. (1982), "A new definition of shape similarity", *Pattern Recognition Letter*, Vol. 1, pp. 87-120.

Parui, S.K. and Majumder, D.D. (1983), "Symmetry analysis by computer", *Pattern Recognition*, Vol. 16, pp. 63-7.

Rosenfeld, A. (1970), "A non-linear edge detection", *Proc. IEEE*, Vol. 58, pp. 814-16.

Shafer, G. (1996), *A Mathematical Theory of Evidence*, Princeton, NJ.

Steven, A.L., Zucker, W. and Rosenfeld, A. (1977), "Iterative enhancement of noisy images", *IEEE transaction on SMC*, *SMC*, Vol. 7, pp. 435-42.

Tahoves, P.G. *et al.* (1991), "Enhancement of chest and breast radiographs by automatic spatial filtering", *IEEE Trans. on Medical Imaging*, Vol. 20 No. 4, pp. 330-35.

Van den Elsen *et al.* (1993), "Medical image matching – a review with classification", *IEEE Trans. Engg. Med. Bio.*, pp. 26-39.

von Foerster, H. (1981), *Observing Systems*, Inter Systems Publications, Sea Side, CA.

Wiener, N. (1984), *Cybernetics*, The MIT Press and John Wiley & Sons Inc. New York, NY.